HHS Public Access

Author manuscript

Cell Rep. Author manuscript; available in PMC 2017 September 20.

Published in final edited form as:

Cell Rep. 2017 August 29; 20(9): 2044–2056. doi:10.1016/j.celrep.2017.08.020.

NEIL3 repairs telomere damage during S phase to secure chromosome segregation at mitosis

Jia Zhou[*,1,3,5], **Jany Chan**[*,1], **Marie Lambelé**[1], **Timur Yusufzai**[5], **Jason Stumpff**[2,3], **Patricia L. Opresko**[4], **Markus Thali**[**,1,3], and **Susan S Wallace**[**,1,3,6]

[1]Department of Microbiology and Molecular Genetics, College of Medicine and College of Agriculture and Life Sciences, University of Vermont, Burlington, VT 05405

[2]Department of Molecular Physiology and Biophysics, College of Medicine, University of Vermont, Burlington, VT 05405

[3]Graduate Program in Cell and Molecular Biology, University of Vermont, Burlington, VT 05405

[4]Department of Environmental and Occupational Health, University of Pittsburgh Graduate School of Public Health, Hillman Cancer Center, Pittsburgh, PA 15213

[5]Department of Radiation Oncology, Dana-Farber Cancer Institute; Department of Biological Chemistry & Molecular Pharmacology, Harvard Medical School, Boston, MA, 02115

SUMMARY

Oxidative damage to telomere DNA compromises telomere integrity. We recently reported that the DNA glycosylase NEIL3 preferentially repairs oxidative lesions in telomere sequences *in vitro*. Here, we show that loss of NEIL3 causes anaphase DNA bridging due to telomere dysfunction. NEIL3 expression increases during S phase and reaches maximal levels in late S/G2. NEIL3 co-localizes with TRF2, and associates with telomeres during S phase and this association increases upon oxidative stress. Mechanistic studies reveal that NEIL3 binds to single-stranded DNA via its intrinsically disordered C-terminus in a telomere sequence-independent manner. Moreover, NEIL3 is recruited to telomeres through its interaction with TRF1, and this interaction enhances the enzymatic activity of purified NEIL3. Finally, we show that NEIL3 interacts with APE1 and the long patch base excision repair proteins PCNA and FEN1. Taken together, we propose that NEIL3

[**]Corresponding authors: Susan S. Wallace, 201 Stafford Hall, 95 Carrigan Drive, Burlington, VT 05405, Telephone: 802 656-2164, Fax: 802 656-8749, Susan.Wallace@uvm.edu, Markus Thali, 318 Stafford Hall, 95 Carrigan Drive, Burlington, VT 05405, Telephone: 802-656-1056, Fax: 802-656-8749, Markus.Thali@uvm.edu.

[6]Lead Contact

[*]These authors contributed equally to this study

Supplemental Information

Supplemental Information includes 7 figures, 4 videos and Experimental Procedures.

AUTHOR CONTRIBUTIONS

JZ, JC, TY, JS, PLO, MT and SSW designed the experiments.

JZ, JC and ML conducted the experiments and acquired and analyzed the data.

JZ, JC, JS, PLO, MT and SSW contributed to the writing and editing of the manuscript.

TY, PLO and JS provided critical reagents.

protects genome stability through targeted repair of oxidative damage in telomeres during S/G2 phase.

Graphical abstract

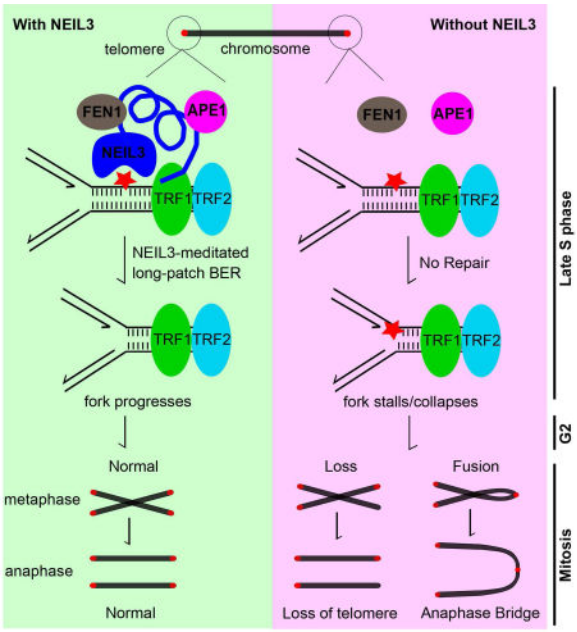

Keywords

NEIL3 glycosylase; telomere; mitotic defects; DNA repair

INTRODUCTION

The ends of mammalian chromosomes are capped by telomeres that prevent chromosome ends from being misidentified as broken DNA strands. The shelterin complex, which contains the telomere binding proteins TRF1, TRF2, and POT1 (Palm and de Lange, 2008), shields telomeres from recognition by DNA damage response (DDR) proteins, making telomeres refractory to DNA repair (Fumagalli et al., 2012; Karlseder et al., 1999). However, guanine has the highest oxidation potential of the nucleotides and is especially susceptible to oxidation in tandem or repeat sequences (Oikawa and Kawanishi, 1999). Therefore, the G-rich telomere repeats in proliferating cells are exceptionally vulnerable to reactive oxygen species that result from normal metabolic processes (Liu et al., 2002). When exposed to oxidative stress under *in vivo* or *in vitro* conditions, telomeres harbor more DNA lesions than other regions of the genome (Hewitt et al., 2012; Wang et al., 2010). If left unrepaired, these oxidative lesions may compromise the binding of shelterin proteins to telomere DNA (Opresko et al., 2002) or lead to telomere defects and eventually apoptosis (Deng et al., 2008; Liu et al., 2002). Furthermore, telomere dysfunction has been shown to contribute to the initiation and progression of tumorigenesis as demonstrated by telomere erosion, DNA bridging, and chromosomal instability in colon, prostate, and breast cancers (Chin et al., 2004; Meeker et al., 2002; Rudolph et al., 2001).

Most oxidative lesions are repaired by the base excision repair (BER) pathway (Dianov and Lindahl, 1994). BER is initiated by a DNA glycosylase that excises damaged bases, resulting in apurinic/apyrimidinic (AP) sites. The recruitment of downstream BER proteins results in cleavage of the AP site by an endonuclease (i.e. AP Endonuclease 1 or APE1), gap filling by a DNA polymerase and ligation by a DNA ligase, thus restoring the original sequence (for reviews see (Hegde et al., 2008; Wallace, 2014)). BER can be divided into short-patch (SP-BER) and long-patch (LP-BER) sub-pathways based on the enzymes involved and the size of newly synthesized DNA insert. Polymerase β and DNA ligase III are involved in short-patch BER (SP-BER) (Dianov and Lindahl, 1994; Kubota et al., 1996), which typically entails the excision of a single nucleotide, whereas long-patch BER (LP-BER) utilizes the PCNA-dependent replicative polymerases, a flap DNA endonuclease FEN1, and DNA ligase I to replace a stretch of 2–20 nucleotides (Fortini et al., 1998; Klungland and Lindahl, 1997). Interestingly, expression of LP-BER genes is enriched during S phase, whereas SP-BER genes are equally expressed in all cell cycle phases (Mjelle et al., 2015). Furthermore, LP-BER enzymes, including FEN1, are recruited to telomeres through an interaction with the telomere-associated proteins TRF1 and TRF2, which have been shown to have a stimulatory effect on LP-BER (Fotiadou et al., 2004; Miller et al., 2012; Muftuoglu et al., 2006).

NEIL3 is a member of the Nei-like (NEIL) DNA glycosylase family, which also includes NEIL1 and NEIL2. NEIL1 and NEIL2 have an overlapping function with the housekeeping DNA glycosylase NTH1 but can also initiate BER during specific processes: NEIL1 acts during DNA replication while NEIL2 associates with active transcription sites (Dou et al., 2003; Hegde et al., 2013). Currently, the cellular functions of NEIL3 are only beginning to be understood. NEIL3 is distinguished from the other NEILs by an exceptionally long intrinsically disordered CTD, which doubles the size of the protein (Liu et al., 2010; Liu et al., 2012). Although we have characterized the NEIL3 glycosylase domain *in vitro* and showed it to prefer lesions in single-stranded DNA (ssDNA) and quadruplex DNA over duplex DNA (Krokeide et al., 2009; Liu et al., 2010; Liu et al., 2012; Zhou et al., 2013), the function of its large CTD remains unknown.

The NEIL3 DNA glycosylase is an intriguing candidate for repairing oxidative damage in telomeric sequences in proliferating cells. DNA glycosylases have been implicated in protecting telomere integrity (Vallabhaneni et al., 2013; Wang et al., 2010), and we recently showed that the purified glycosylase domain of NEIL3 preferentially removes oxidative lesions from telomere DNA (Zhou et al., 2013). We also showed NEIL3 to excise lesions from telomere G-quadruplexes, DNA structures that are normally inhibitory to DNA processing enzymes (Fleming et al., 2015; Zhou et al., 2015; Zhou et al., 2013). Moreover, expression of NEIL3 is restricted to cells with a high proliferative capacity, such as adult/embryonic stem cells and hematopoietic cells (Reis and Hermanson, 2012; Torisu et al., 2005), while NEIL3 expression is repressed in non-dividing cells (Neurauter et al., 2012). In adult humans, NEIL3 transcripts are only detectable in the thymus and testes (Morland et al., 2002; Torisu et al., 2005), whereas in mice, transcripts are also present in the spleen, bone marrow, and regenerative subregions of the brain (Hildrestrand et al., 2009; Torisu et al., 2005). Interestingly, *Neil3* nullizygous mice display proliferation defects in several adult stem/progenitor cell populations (Hildrestrand et al., 2009; Regnell et al., 2012; Rolseth et

al., 2013; Torisu et al., 2005), while expression of NEIL3 is significantly elevated in sixteen cancerous tissues (Hildrestrand et al., 2009). In addition, we recently showed that splenic T and B cells as well as germinal center B cells from *Neil3*$^{-/-}$ mice suffer increased apoptosis and cell death (Massaad et al., 2016). Taken together, these data suggest that NEIL3 may play an essential role in protecting telomere integrity in actively dividing cells.

Here, we report a thorough spatiotemporal study of NEIL3 localization during the cell cycle, and identify a novel, mechanistic link between NEIL3-dependent DNA repair and telomere integrity. To ensure genomic stability, NEIL3 specifically repairs DNA damage in telomeres during late S phase, presumably through the LP-BER pathway. Furthermore, we identify several important protein-protein interactions involving the intrinsically disordered C-terminal domain of NEIL3 with TRF1, and LP-BER proteins. Our results rationally explain the upregulation of NEIL3 in many highly proliferative cell types, including cancer cells.

RESULTS

Ablation of NEIL3 results in a prolonged metaphase and an increase in anaphase DNA bridges

Several studies show that NEIL3 plays a critical role in proliferating cells (Hildrestrand et al., 2009; Reis and Hermanson, 2012; Torisu et al., 2005). We thus asked whether NEIL3 is essential for cell proliferation and examined the consequences of NEIL3 depletion in cells. We first attempted to generate stable knockdown cell lines. Despite utilizing multiple approaches and cell types, we were unable to recover NEIL3 knockdown cells following selection, which supports previous data showing that NEIL3 is essential in proliferating cells (Reis and Hermanson, 2012; Sejersted et al., 2011). We then attempted to transiently reduce NEIL3 levels using a panel of five siRNAs. The most efficient siRNA with minimal off target effects was then used in the subsequent experiments. The efficiency of knockdown was first confirmed by Western blotting (Figure 1A) of synchronized HCT116 cells at S and G2/M phases (3 and 6 hours after release from double thymidine block, T3 and T6, respectively), where NEIL3 showed high expression. siNEIL3-treated cells contained much lower NEIL3 protein than the control siRNA-treated cells at both time points tested (Figure 1A). We later confirmed the knockdown by measuring the mean fluorescence intensity (MFI) of NEIL3 relative to α-tubulin in metaphase cells (Figure 4F).

To assess whether the timing of mitosis was affected when NEIL3 was transiently depleted, we utilized time-lapse microscopy to image actively dividing HCT116 cells stably expressing GFP-H2B treated with scramble or NEIL3 siRNA (Figure 1B–C). While untreated and scramble siRNA-treated cells progressed through mitosis (from DNA condensation to chromatid separation) at a similar rate (49±18 min and 45±21 min, Figure 1B–C; Videos 1 and 2), a reduction in NEIL3 levels typically led to metaphase arrest prior to attempting to complete mitosis (179±121 min; Figure 1B–C). The majority of the siNEIL3-treated cells (70%) displayed aberrant mitoses, with 52% arrested during metaphase and then undergoing apoptosis while the remaining 18% displayed an extended metaphase delay (i.e. longer than 45 min) before completing mitosis (Figure 1D; Videos 3 and 4, respectively). We also observed an increase in DNA bridging during anaphase in knockdown

cells compared to untreated and scramble siRNA-treated cells but no significant effect on chromosome fragmentation (Figure 1E).

Knockdown of NEIL3 increases telomere dysfunction

Our recent studies show that NEIL3 preferentially removes damaged bases from telomere DNA and telomere G-quadruplexes *in vitro* (Fleming et al., 2015; Zhou et al., 2015; Zhou et al., 2013). We hypothesized that the mitotic defects observed after NEIL3 knockdown (Figure 1) could be due to dysfunctional telomeres resulting from a failure in DNA repair. We therefore compared the number of telomere defects in metaphase spreads of siNEIL3- and control siRNA-treated HCT116 cells using telomere fluorescence *in situ* hybridization (FISH) (Figure 2). NEIL3 was successfully knocked down by two siRNA (siNEIL3-B and siNEIL3-C, Figure 2A). Telomeres were visualized with a Cy3-labeled peptide nucleic acid (PNA) probe against the G-strand (Figure 2B). Telomere loss, telomere fusion between sister chromatids, extra telomere signals, and telomere associations between chromosomes were identified from deconvolution micrographs (Figure 2C). Upon NEIL3 knockdown, we observed a 2-fold increase in telomere loss and sister chromatid fusions as well as significant increases in extra telomere signals and chromosome association in comparison to scramble-treated cells (Figure 2D).

To examine whether chronic NEIL3 loss also leads to telomere defects, we performed the telomere FISH experiments in primary mouse embryonic fibroblasts (MEFs) from *Neil3* knock out and WT control mice. We found that the *Neil3*$^{-/-}$ cells presented similar telomere defects to those observed in NEIL3-depleted HCT116 cells. The *Neil3*$^{-/-}$ cells develop more telomere loss, duplication and fusions than littermate-matched WT control cells (Figure S6A–B). To test if the enzymatic activity of NEIL3 is required for telomere protection, we examined the telomeres of primary human fibroblasts from a patient with a NEIL3 D132V mutation, which abolishes the glycosylase activity of NEIL3 (Massaad et al., 2016). We observed a more than 2-fold increase in telomere loss in the D132V cells from the patient, compared to the WT control cells from the patient's healthy sibling (Figure S6C). However, we did not find a difference in telomere duplication or fragile telomeres between the D132V mutant and WT cells. Together, we conclude that chronic loss of *Neil3* leads to telomere defects and that the catalytic activity of NEIL3 is required, at least in part, to protect telomeres.

To determine whether the telomere defects we observed upon NEIL3 knockdown were caused by telomere dysfunction, telomere dysfunction induced foci (TIF) assays were performed. TIFs were visualized and identified as the 53BP1 foci that co-localized with TRF2 foci (Figure 2E). We observed a clear increase of TIFs in two NEIL3 siRNA-treated groups compared to the control siRNA-treated cells (Figure 2F). Together, these data show that the reduction in NEIL3 levels correlates with an increase in telomere dysfunction, which leads to metaphase arrest, increased DNA bridging during anaphase, and ultimately decreased cell proliferation.

NEIL3 expression increases during S phase and reaches maximal levels during G2/M in cancer cell lines and primary CD4$^+$ lymphocytes

To better understand the role that NEIL3 plays in protecting telomere integrity, we examined the expression profile and subcellular localization of NEIL3 throughout the cell cycle. We first used flow cytometry to assess NEIL3 protein levels during different phases of cell division, utilizing the well-characterized HeLa cell line. Cells were synchronized at early S phase using a double thymidine block, and NEIL3 was immunoprecipitated from cell lysates at the indicated time points following release (Figure 3A). Cells displayed a high degree of synchronization through the first cell division (approximately 14–16 h; Figure 3B). NEIL3 (~68 kDa) was undetectable immediately after release into S phase and reached maximal levels six hours post-release (Figure 3C), which corresponds to the late S/G2 phase (Figure 3B). On average, NEIL3 levels increased five-fold above basal levels when normalized to GAPDH (Figure 3C). Unlike previously published results (Neurauter et al., 2012), we did not detect NEIL3 during early S phase in HeLa cells, which corresponds to time point T0. This discrepancy may be due to differences in cell lines (cancer cells versus fibroblasts) and the methods used for synchronization (double thymidine block versus serum starvation).

Since induction of cell synchrony can perturb signaling and transcriptional pathways, we also analyzed the MFI of NEIL3 relative to DNA content in asynchronous cultures by flow cytometry (Figure 3D–E; for gating schemes, see Figure S1B). We also expanded our studies from HeLa cells to CEMss and Jurkat cell lines (CD4$^+$ T lymphocytes derived from lymphoblastic leukemias) and activated primary CD4$^+$ T cells from healthy donors. In all four cell types, NEIL3 displayed the highest MFI in cells containing a relative 4N DNA content (G2/M; Figure 3D–E), which corroborated both our microscopy and immunoprecipitation data. The two T lymphocyte lines, CEMss and Jurkat, as well as the primary CD4$^+$ T cells exhibited a higher overall NEIL3 signal compared to HeLa cells, but we again observed that the highest MFI occurred in the G2/M subpopulation (Figure 3D). Based on these data, we conclude that NEIL3 may initially function during late S phase and into G2, which correlates well with the final steps of telomeric DNA synthesis and end processing into capped structures (Verdun and Karlseder, 2006; Zhao et al., 2009).

NEIL3 localizes to the interphase nucleus and is sequestered to spindle microtubules during mitosis

We next analyzed the spatiotemporal localization of NEIL3 in HeLa cells and T lymphocytes (Figure 4). In HeLa cells, we observed two distinct immunofluorescence staining patterns for NEIL3 during interphases. In the majority of cells, little to no NEIL3 signal was detectable (Interphase 1; Figure 4A). A smaller population of interphase cells presented a high intensity, speckled pattern in the nucleus (Interphase 2; Figure 4A). Upon entry into mitosis, the nuclear NEIL3 signal dissociated from the condensing DNA in prophase and re-localized to the mitotic spindle. As cells transitioned from anaphase to telophase, the NEIL3 signal shifted to the central spindle and then accumulated at the intercellular bridge and abscission zone (bottom row; Figure 4A). Interestingly, although sharing a relatively similar localization during cytokinesis, NEIL3 did not display significant co-localization with Aurora B on the central spindle or the intercellular bridge (Figure S4A, middle and right panels). Instead, the Aurora B signal preceded NEIL3 along the central

spindle before accumulating at the abscission zone. Similar spatiotemporal localizations were observed in CEMss cells (Figure 4B) and activated primary $CD4^+$ T cells (Figure 4C). We confirmed the NEIL3 localization using three antibodies generated against N-terminal or C-terminal epitopes as well as using different fixation methods, including methanol, glutaraldehyde, and paraformaldehyde, indicating that these localizations were not an artifact of sample preparation (Figure S1A and data not shown).

During mitosis, NEIL3 exhibited a strong co-localization with microtubules of the mitotic and central spindle ($r = 0.62 \pm 0.33$; Figure 4D). To further confirm the localization of NEIL3 during mitosis and validate the specificity of our siRNAs, mitotic NEIL3 staining of siNEIL3- or scramble siRNA-treated HCT116 cells was performed, and we observed a specific and effective reduction of NEIL3 signal during metaphase (Figure 4E–F). Knockdown of NEIL3 did not affect spindle organization nor was centrosome replication or positioning perturbed (Figure 4E). Taken together, these data indicate that NEIL3 is not involved in DNA processes during mitosis, since the NEIL3 signal re-localized away from the condensing DNA to spindle microtubules during the G2/M transition. We conclude that the telomere defects and the abnormalities in chromosome separation in NEIL3-deficient cells are due to events that occurred in late S-phase or G2 prior to mitosis.

NEIL3 localization to telomeres is enhanced after oxidative stress during late S phase

To understand how NEIL3 promotes telomere stability prior to mitosis, we first asked if NEIL3 localizes to telomeres using immunofluorescence imaging. U2OS cells were used in these experiments because of their long average telomere lengths, which yield enhanced signals of TRF2 foci staining and therefore, potentially NEIL3 foci. We observed that NEIL3 foci co-localized with the telomere marker TRF2 in U2OS cells (Figure 5A and Figure S2), with 58.4% of NEIL3 foci overlapping TRF2 foci. To exclude the possibility of cross-reactivity of secondary antibodies, a different set of secondary antibodies was used to perform the same experiments, and similar results were observed (Figure S3), with 66.5% of NEIL3 foci overlapping TRF2 foci. We thus conclude that NEIL3 localizes to telomeres in U2OS cells. We also performed immunofluorescence in HeLa cells that possess shorter telomeres compared to U2OS cells; however, we were not able to analyze co-localization in HeLa cells due to low signal intensities in both channels (data not shown). To exclude the possibility that the telomere localization of NEIL3 is specific to telomerase-negative cells (such as U2OS cells), we performed the colocalization experiments with the telomerase-positive glioblastoma cell line T98G. We did observe partial colocalization of NEIL3 with TRF1 in T98G cells, although the colocalization was not as great as in U2OS cells (Figure S7A–B), with 31.7% of NEIL3 foci overlapping TRF1 foci.

Using chromatin immunoprecipitation (ChIP), we then asked if NEIL3 directly associates with telomeres. We utilized quantitative PCR (qPCR) to analyze the enrichment of NEIL3 to telomeres in ChIP samples (Figure 5B–D). HeLa cell proteins were cross-linked 6 hours after a thymidine block when cells are in late S/G2. TRF2 and H3 antibodies were used as telomere-specific and telomere-non-specific positive controls for ChIP and qPCR (see Materials and Methods for details). The TRF2 antibody showed highly specific ChIP with telomere DNA, indicating that the ChIP/qPCR method is suitable for analysis of telomere

association (Figure 5B). We found that the amount of telomere DNA, but not Alu DNA, was significantly higher in NEIL3 ChIP samples compared to negative controls. In addition, the amount of telomere DNA was much higher than Alu DNA in the NEIL3 ChIP samples, indicating a specific enrichment of NEIL3 at telomeres compared to other repetitive sequences (Figure 5B).

We previously showed that NEIL3 preferentially recognizes DNA base damages (thymine glycol and 5-OHU) in the context of telomere sequences and efficiently removes base damages from telomere quadruplex DNA (Zhou et al., 2015; Zhou et al., 2013). Based on these results and our current observations, we asked whether NEIL3 directly functions in repair of oxidative damage at telomeres. We synchronized HeLa cells and treated them with H_2O_2 during S phase, and then ChIP experiments were performed on lysates harvested during late S/G2 phase. We observed the same ChIP pattern in the H_2O_2-treated samples as in the untreated samples: NEIL3 was enriched in telomeres but not Alu elements (Figure 5C). Importantly, there was a greater than two-fold enrichment of telomere DNA in NEIL3 ChIP samples following H_2O_2 treatment compared to the untreated samples (compare first columns of Figure 5C to 5B). In addition, this enrichment of NEIL3 to telomere DNA was dose-dependent in response to H_2O_2 concentration (Figure 5D). Of note, NEIL3 also became detectable at Alu sequences after H_2O_2 treatment; however, the level of NEIL3 present at the Alu sequence was much lower than at the telomere sequence, and it was not dependent on H_2O_2 dose. These data demonstrate that NEIL3 localization to telomeres is enhanced upon oxidative stress, implying that NEIL3 is recruited to telomeres to repair oxidative damage during S phase.

NEIL3 interacts with TRF1 and binds ssDNA in a non-telomere-specific manner

Next, we addressed how NEIL3 is recruited to telomeres. One possibility is that NEIL3 binds to telomere DNA specifically. To test this hypothesis, DNA pulldown assays were carried out using biotin-labeled DNA with different sequences and structures. As shown in Figure 6B, endogenous NEIL3 from HeLa whole cell lysates was able to bind telomere ssDNA and G-quadruplex DNA but not double-stranded DNA. However, the binding was not telomere sequence-specific, since NEIL3 also bound to a random sequence DNA (ssR). To confirm this, we tested if the HA-tagged full length NEIL3, the N-terminal glycosylase domain (N-terminus, aa1–281, refer to the domain map in Figure 6A), or the intrinsically disordered CTD (C-terminus, aa282–605) associated with double-stranded, ssG or ssC telomere sequences (Figure 6C). The HA-tagged full length NEIL3 and the CTD alone were readily pulled down by biotinylated ssDNA mimicking G-strand and C-strand telomere sequences but they bound very weakly to double-stranded telomere DNA. We did not detect any DNA binding by the HA-tagged N-terminal construct. Together, these data suggest that NEIL3 is capable of binding telomere DNA via its CTD but the binding is not telomere sequence-specific, indicating that other mechanisms are involved in the specific enrichment of NEIL3 to telomeres.

We then tested if protein-protein interactions were mediating the recruitment of NEIL3 to telomeres. We focused on components of the shelterin complex, specifically TRF1, TRF2, and POT1, which bind specifically and directly to telomere DNA. Using co-

immunoprecipitation experiments, we detected an interaction between NEIL3-HA and TRF1 but not with TRF2 or POT1 (Figure 6D). The TRFH domains of TRF1 and TRF2 have been reported to mediate multiple protein-protein interactions that include the TIN2-TRF1 interaction (Chen et al., 2008). To understand if the NEIL3-TRF1 interaction is mediated by the TRFH domain, we performed the co-IP in extracts of transiently transfected HEK293 cells. We found that NEIL3 interacted with wild type TRF1 but not the TRFH mutant F142A (Figure 6E), which has been shown to abolish TIN2 interaction (Chen et al., 2008). Although NEIL3 co-immunoprecipitated with TRF1 but not TRF2, when we switched the TRFH domain of TRF2 with that of TRF1 (chimeric TRF2, TRFcT), we now observed the chimeric TRF2, TRFcT, to interact with NEIL3 (Figure S5A–B). These data indicate that NEIL3 specifically interacts with TRF1 through its TRFH domain.

To confirm this result and assess whether this interaction was mediated by the N-terminal or the C-terminal domain of NEIL3, we tested the protein interactions using a modified Far-Western technique. The strongest interaction with TRF1 occurred in the context of the full-length protein when the CTD is present (NEIL3-FL), although we did observe a weak interaction with the glycosylase domain alone (NEIL3-GD, Figure 6F). The interaction is also unique to NEIL3, since no interactions with NEIL1 or NEIL2 were detected under the same conditions (Figure 6F). The CTD alone could not be tested, since we are not able to purify the disordered CTD. These results support a model where NEIL3 is recruited to telomeres by a CTD-dependent interaction with TRF1.

Finally, we asked if the recruitment of NEIL3 to telomeres was TRF1 dependent in cells. We used the glioblastoma cell line T98G, and TRF1 knock down and ChIP were carried out. The knockdown was very efficient as confirmed by immuno-staining (Figure S5C). Moreover, after TRF1 knockdown, there was a 5.2-fold decrease of NEIL3-bound telomere DNA. Although the NEIL3-bound Alu DNA also showed a decrease after TRF1 knockdown, the difference was smaller (2.9-fold). Also, NEIL3 bound telomere DNA much better than the Alu sequence when TRF1 was present; however, when TRF1 was knocked down, NEIL3 bound both sequences similarly. These results not only show clearly that the recruitment of NEIL3 to telomeres is TRF1-mediated, but also demonstrate that NEIL3 selectively binds to telomeres independently of cell-type.

The C-terminal domain is required for maximal NEIL3 activity and interacts with LP-BER components

Since components of the shelterin complex have been shown to stimulate the LP-BER pathway (Fotiadou et al., 2004; Miller et al., 2012; Muftuoglu et al., 2006), we next assessed whether the interaction between the NEIL3 CTD and TRF1 affected the enzymatic activity of NEIL3. We quantified the activity of purified full length NEIL3 (NEIL3-FL; Figure 7A, 7C) or the glycosylase domain alone (NEIL3-GD; Figure 7B, 7D) in the presence or absence of TRF1. Since TRF1 specifically binds double-stranded telomere DNA, we utilized duplex telomere DNA with the oxidative lesion guanidinohydantoin (Gh) as the substrate. The catalytic activity of full-length NEIL3 was higher in the presence of TRF1 (Figure 7C). However, in the absence of the CTD, TRF1 strongly inhibited the activity of the NEIL3 glycosylase domain (Figure 7D). In these reactions, the ratio of DNA substrate:TRF1:NEIL3

was 1:20:20. We also tested the ratio of 1:10:4, and found TRF1 to stimulate the activity of NEIL3 under this condition as well (Figure S7C–D). Thus, our data show that the intrinsically disordered CTD is required for maximal activity of NEIL3 on TRF1-bound telomere DNA. However, without testing all reaction conditions, there is a possibility that NEIL3 may have an additional role, independent of its enzymatic activity, in protecting telomeres. This is also suggested by the milder phenotype observed in D132V mutant cells compared to the NEIL3 knockout cells (Figure S6).

Since LP-BER enzymes are enriched specifically in S-phase (Mjelle et al., 2015) when NEIL3 expression is also high, we examined if NEIL3 functions in concert with other LP-BER enzymes. We tested a panel of BER proteins for their interaction with NEIL3 by co-immunoprecipitation (Figure 7E). Using NEIL3-HA, we detected an interaction between NEIL3 and the LP-BER proteins, PCNA and FEN1. In contrast, we did not detect an interaction between NEIL3 and polymerase β, which is the polymerase that primarily functions in SP-BER. In addition, we also observed an interaction with the AP endonuclease APE1 but not with APE2 (Figure 7E). Since NEIL3 has a weak lyase activity (Krokeide et al., 2013; Liu et al., 2010), this interaction may be important in mediating cleavage of the DNA strand for efficient repair of telomere damages.

Next, we confirmed these interactions and mapped the interaction domain in NEIL3 by Far-Western analysis (Figure 7F). NEIL1 and NEIL2 glycosylases were included as controls. Endogenous PCNA and FEN1, but not APE1, were detected in association with purified NEIL1 as well as NEIL2 but with weaker affinity, which agrees with previous reports (Das et al., 2006; Hegde et al., 2013; Wiederhold et al., 2004). Using this technique, we confirmed that NEIL3 interacts with PCNA, FEN1, and APE1 (Figure 7F), which confirms the co-IP data (Figure 7E). Additionally, we revealed that PCNA and FEN1 associated with the glycosylase domain and full-length NEIL3 (NEIL3-GD and NEIL3-FL), suggesting an interaction with the N-terminus of NEIL3. However, the full-length NEIL3 interacts with APE1 strongly while the glycosylase domain only binds to APE1 weakly, indicating that this interaction is primarily mediated by the NEIL3 CTD (Figure 7F). Together, our data demonstrate that NEIL3 interacts directly with downstream LP-BER enzymes and indicate that NEIL3 can protect telomeres from oxidative damage by initiating LP-BER at telomeres.

DISCUSSION

We recently found that splenic T and B cells as well as germinal center B cells from *Neil3*$^{-/-}$ mice display a marked increase in apoptosis and cell death and, as a result, increased predisposition to autoimmunity (Massaad et al., 2016). Our current study reveals an essential role for NEIL3 in protecting telomere integrity by coordinating repair of oxidative damage in actively dividing cells. We provide evidence that the absence of NEIL3 in proliferating cells results in telomere dysfunction that contributes to the formation of DNA bridges, aberrant mitoses, and consequent cell death. Based on our data, we propose the following model for NEIL3 cellular function. NEIL3 is targeted to telomeres through a CTD-dependent interaction with the TRFH domain of TRF1 during late S- and G2- phases when NEIL3 levels are elevated. NEIL3 initiates DNA repair of oxidative damage and subsequently recruits APE1, FEN1 and PCNA to complete the repair process, presumably

via long-patch BER. Finally, as cells transition into mitosis, NEIL3-dependent repair is inhibited by sequestering the protein to the mitotic spindle.

While genomic DNA is readily repaired, telomeres appear to be refractory to DDR and DNA repair pathways due to their highly repetitive sequences, associated proteins, and unique structures (reviewed (Fouquerel et al., 2016)). Specifically, the G-strand telomere DNA can form inhibitory secondary structures termed G-quadruplex DNA (Lipps and Rhodes, 2009). In biochemical assays, NEIL3 is one of the two DNA glycosylases that can remove oxidized bases from G-quadruplex DNA structures (Fleming et al., 2015; Zhou et al., 2015; Zhou et al., 2013). Following oxidative damage, G-quadruplex structures can form and "loop out" the damaged ssDNA region thus making it an ideal substrate for NEIL3 (Fleming et al., 2015). Furthermore, the catalytic domain of NEIL3 contains a DNA binding pocket that can accommodate a broad spectrum of damages (Liu et al., 2010; Liu et al., 2013). These biochemical features suit NEIL3 well for its role in telomere repair. We propose that the flexibility of NEIL3 to repair multiple forms of telomere DNA, its broad lesion specificity, and its preference for telomere sequences make this enzyme an ideal candidate for initiating BER at telomeres.

BER enzymes have been reported to function in telomere protection, primarily in yeast and mouse cells. DNA polymerase β interacts with TRF2 and induces telomere dysfunction when ectopically expressed in a murine mammary cell line (Fotiadou et al., 2004). *Nthl1*$^{-/-}$ mice suffer from telomere attrition and increased recombination, DNA damage foci and fragile telomere sites in bone marrow cells (Vallabhaneni et al., 2013). In Ogg1-deficient mouse cells, altered telomere length was observed (Wang et al., 2010). It appears that depletion of BER enzymes generally deteriorates telomere homeostasis. However, the phenotype we observed after NEIL3 knockdown was more severe than the reported effects of Nthl1 and Ogg1 depletion. The targeted telomere repair of NEIL3 as well as its broad substrate specificity (Liu et al., 2010; Liu et al., 2013; Zhou et al., 2013) may account for its importance in maintaining telomere integrity. Moreover, the major human endonuclease APE1 plays an important role in telomere maintenance (Madlener et al., 2013). Interestingly, NEIL3 interacts with APE1 (Figure 7E), and we found that NEIL3 colocalizes with APE1 at anaphase bridges (Figure S4B–D). These data suggest that the two may share a common mechanism to protect genome stability, that is, to keep telomeres base-damage free and potentially resolve anaphase bridges. Our current study not only highlights the importance of BER enzymes in telomere maintenance but also provides a more detailed mechanism as to how a DNA glycosylase functions at telomeres.

TRF1 and TRF2 are scaffolding proteins that bind specifically to telomere duplex DNA and recruit a number of DNA repair enzymes to telomeres, including the non-homologous end joining (NHEJ) protein Ku (Chen et al., 2008; de Lange, 2002) and BER enzymes polymerase β and FEN1 (Fotiadou et al., 2004; Muftuoglu et al., 2006). Our study here shows that NEIL3 can also be targeted to telomeres through a TRF1-dependent interaction via disordered CTD of NEIL3 with the TRFH domain of TRF1 (Figure 6E and Figure S5A–B). Furthermore, this interaction with TRF1 is necessary for the optimal activity of NEIL3 on duplex telomere DNA. The mechanism for how NEIL3 accesses shelterin-protected damages may be unique to NEIL3, since other DNA glycosylases do not have such a large

CTD. Although NEIL1 has a short CTD that is known to recruit interacting proteins (Hegde et al., 2013), we showed that NEIL1 does not bind to TRF1 (Figure 6F). In addition, NEIL3 expression is cell cycle regulated and elevated in late S-phase, during which time the LP-BER enzymes are the most abundant (Mjelle et al., 2015). Both TRF1 and TRF2 have been shown to promote LP-BER in the telomere DNA context (Miller et al., 2012). These lines of evidence strongly suggest that NEIL3 initiates LP-BER of oxidative damages in telomeres.

Although our data do not directly allow us to determine if NEIL3 depletion leads to TRF1/TRF2 disruption, it is a possible mechanism. Loss of TRF2 causes telomere fusion and anaphase bridging (van Steensel et al., 1998). We and others have previously shown that loss of BER enzymes increases oxidative damages in telomere DNA and therefore attenuates TRF2 and TRF1 binding (Opresko et al., 2005; Vallabhaneni et al., 2013). Also, the interaction of NEIL3 with TRF1 may prevent telomere fusions by limiting double strand breaks in telomeres. Oxidative base damages can block polymerases and cause replication folk stalling that leads to double-strand breaks (Aller et al., 2007). In addition, excessive base damages may cause secondary double strand breaks, if closely placed on opposite strands (Yang et al., 2004). NEIL3, through its interaction with TRF1, may prevent accumulation of base damages and thus double strand breaks in telomeres. In support with this hypothesis, our TIF assay data show that depletion of NEIL3 by siRNA leads to increased 53BP1 foci formation at telomeres (Figure 2E–F), suggesting an increase of NHEJ between telomere ends.

Our findings may also have broader implications in cancer biology. Expression of NEIL3 is up-regulated in sixteen human cancer tissues (Hildrestrand et al., 2009) and is associated with progression to metastasis (Kauffmann et al., 2008). Our data provide an explanation for these observations. Upon NEIL3 knockdown, we report a significant increase in mitotic defects due to telomere dysfunction, including telomere fusion, translocation, and loss. Together with our finding that NEIL3 is directly recruited to telomeres, we conclude that in highly proliferative cell types, reduction of NEIL3 is sufficient to disrupt telomere homeostasis and ultimately leads to telomere defects and cell cycle arrest, emphasizing the role of NEIL3 in protecting telomere integrity. Also, a recent study revealed NEIL3 as a novel enzyme capable of unhooking DNA cross-links during DNA replication (Semlow et al., 2016). Thus, NEIL3 may be an effective drug target for inhibiting tumorigenesis.

In conclusion, our study reveals an essential role for NEIL3 in protecting telomere integrity in proliferating cells. We show that NEIL3 is able to coordinate DNA repair in telomeres with cell cycle progression, and the glycosylase utilizes its CTD to recruit TRF1 and the LP-BER machinery to facilitate repair of telomeres. Taken together, our data provide a rational, mechanistic explanation for the upregulation of NEIL3 in highly proliferative cells under both normal and pathological conditions.

EXPERIMENTAL PROCEDURES

Materials and detailed methods, including antibodies, DNA and RNA constructs, cell culture and synchronization, transient plasmid and siRNA transfections, deconvolution microscopy, time-lapse microscopy, flow cytometry, metaphase spreads and telomere FISH, telomere

dysfunction induced foci (TIF) assays, immunoprecipitation and Western blotting, co-immunoprecipitation and Far-Western blotting, chromatin immunoprecipitation (ChIP) and quantitative PCR (qPCR), DNA pulldown assays, protein purification, glycosylase activity assays and statistical analyses, can be found in Supplemental Information.

Supplementary Material

Refer to Web version on PubMed Central for supplementary material.

Acknowledgments

We thank Dr. Raif S. Geha (Boston Children's Hospital and Harvard Medical School), Dr. Magnar Bjørås (University of Oslo, Norway), and Dr. Ming Lei (Shanghai Institutes for Biological Sciences) for providing *NEIL3-D132V* human fibroblasts, *Neil3*$^{-/-}$ MEFs, and TRF1 expression plasmids, respectively. We thank Joann Sweasy (Yale), David Pederson (UVM), Scott Kathe (UVM), and Menelaos Symeonides (UVM) for helpful discussions. We also thank Heather Galick and April Averill (UVM) for their help in metaphase spread preparation and for purification of glycosylases and Justin Lormand (University of Pittsburgh) for TRF1 purification. This work was supported by NIH grants P01CA098993 (to S.S.W.) from the National Cancer Institute, R01AI080302 and R01GM117839 (to M.T.) from the National Institute of Allergy and Infectious Diseases and National Institute of General Medical Sciences, respectively, P20GM103496-07 (to Budd, R.C., P.I.), and R01ES022944 (to P.L.O.) from the National Institute of Environmental Health Sciences, as well as by an IGP award (to M.T.) from the UVM Larner College of Medicine.

References

Aller P, Rould MA, Hogg M, Wallace SS, Doublie S. A structural rationale for stalling of a replicative DNA polymerase at the most common oxidative thymine lesion, thymine glycol. Proc Natl Acad Sci U S A. 2007; 104:814–818. [PubMed: 17210917]

Chen Y, Yang Y, van Overbeek M, Donigian JR, Baciu P, de Lange T, Lei M. A shared docking motif in TRF1 and TRF2 used for differential recruitment of telomeric proteins. Science. 2008; 319:1092–1096. [PubMed: 18202258]

Chin K, de Solorzano CO, Knowles D, Jones A, Chou W, Rodriguez EG, Kuo WL, Ljung BM, Chew K, Myambo K, et al. In situ analyses of genome instability in breast cancer. Nat Genet. 2004; 36:984–988. [PubMed: 15300252]

Das A, Wiederhold L, Leppard JB, Kedar P, Prasad R, Wang H, Boldogh I, Karimi-Busheri F, Weinfeld M, Tomkinson AE, et al. NEIL2-initiated, APE-independent repair of oxidized bases in DNA: Evidence for a repair complex in human cells. DNA Repair (Amst). 2006; 5:1439–1448. [PubMed: 16982218]

de Lange T. Protection of mammalian telomeres. Oncogene. 2002; 21:532–540. [PubMed: 11850778]

Deng Y, Chan SS, Chang S. Telomere dysfunction and tumour suppression: the senescence connection. Nat Rev Cancer. 2008; 8:450–458. [PubMed: 18500246]

Dianov G, Lindahl T. Reconstitution of the DNA base excision-repair pathway. Curr Biol. 1994; 4:1069–1076. [PubMed: 7535646]

Dou H, Mitra S, Hazra TK. Repair of oxidized bases in DNA bubble structures by human DNA glycosylases NEIL1 and NEIL2. J Biol Chem. 2003; 278:49679–49684. [PubMed: 14522990]

Fleming AM, Zhou J, Wallace SS, Burrows CJ. A Role for the Fifth G-Track in G-Quadruplex Forming Oncogene Promoter Sequences during Oxidative Stress: Do These "Spare Tires" Have an Evolved Function? ACS Cent Sci. 2015; 1:226–233. [PubMed: 26405692]

Fortini P, Pascucci B, Parlanti E, Sobol RW, Wilson SH, Dogliotti E. Different DNA polymerases are involved in the short- and long-patch base excision repair in mammalian cells. Biochemistry. 1998; 37:3575–3580. [PubMed: 9530283]

Fotiadou P, Henegariu O, Sweasy JB. DNA polymerase beta interacts with TRF2 and induces telomere dysfunction in a murine mammary cell line. Cancer Res. 2004; 64:3830–3837. [PubMed: 15172990]

Fouquerel E, Parikh D, Opresko P. DNA damage processing at telomeres: The ends justify the means. DNA Repair. 2016; 44:159–168. [PubMed: 27233113]

Fumagalli M, Rossiello F, Clerici M, Barozzi S, Cittaro D, Kaplunov JM, Bucci G, Dobreva M, Matti V, Beausejour CM, et al. Telomeric DNA damage is irreparable and causes persistent DNA-damage-response activation. Nat Cell Biol. 2012; 14:355–365. [PubMed: 22426077]

Hegde ML, Hazra TK, Mitra S. Early steps in the DNA base excision/single-strand interruption repair pathway in mammalian cells. Cell Res. 2008; 18:27–47. [PubMed: 18166975]

Hegde ML, Hegde PM, Bellot LJ, Mandal SM, Hazra TK, Li GM, Boldogh I, Tomkinson AE, Mitra S. Prereplicative repair of oxidized bases in the human genome is mediated by NEIL1 DNA glycosylase together with replication proteins. Proc Natl Acad Sci U S A. 2013; 110:E3090–3099. [PubMed: 23898192]

Hewitt G, Jurk D, Marques FD, Correia-Melo C, Hardy T, Gackowska A, Anderson R, Taschuk M, Mann J, Passos JF. Telomeres are favoured targets of a persistent DNA damage response in ageing and stress-induced senescence. Nat Commun. 2012; 3:708. [PubMed: 22426229]

Hildrestrand GA, Neurauter CG, Diep DB, Castellanos CG, Krauss S, Bjoras M, Luna L. Expression patterns of Neil3 during embryonic brain development and neoplasia. BMC Neurosci. 2009; 10:45. [PubMed: 19426544]

Karlseder J, Broccoli D, Dai Y, Hardy S, de Lange T. p53- and ATM-dependent apoptosis induced by telomeres lacking TRF2. Science. 1999; 283:1321–1325. [PubMed: 10037601]

Kauffmann A, Rosselli F, Lazar V, Winnepenninckx V, Mansuet-Lupo A, Dessen P, van den Oord JJ, Spatz A, Sarasin A. High expression of DNA repair pathways is associated with metastasis in melanoma patients. Oncogene. 2008; 27:565–573. [PubMed: 17891185]

Klungland A, Lindahl T. Second pathway for completion of human DNA base excision-repair: reconstitution with purified proteins and requirement for DNase IV (FEN1). EMBO J. 1997; 16:3341–3348. [PubMed: 9214649]

Krokeide SZ, Bolstad N, Laerdahl JK, Bjoras M, Luna L. Expression and purification of NEIL3, a human DNA glycosylase homolog. Protein Expr Purif. 2009; 65:160–164. [PubMed: 19121397]

Krokeide SZ, Laerdahl JK, Salah M, Luna L, Cederkvist FH, Fleming AM, Burrows CJ, Dalhus B, Bjoras M. Human NEIL3 is mainly a monofunctional DNA glycosylase removing spiroimindiohydantoin and guanidinohydantoin. DNA Repair (Amst). 2013; 12:1159–1164. [PubMed: 23755964]

Kubota Y, Nash RA, Klungland A, Schar P, Barnes DE, Lindahl T. Reconstitution of DNA base excision-repair with purified human proteins: interaction between DNA polymerase beta and the XRCC1 protein. EMBO J. 1996; 15:6662–6670. [PubMed: 8978692]

Lipps HJ, Rhodes D. G-quadruplex structures: in vivo evidence and function. Trends Cell Biol. 2009; 19:414–422. [PubMed: 19589679]

Liu L, Trimarchi JR, Smith PJ, Keefe DL. Mitochondrial dysfunction leads to telomere attrition and genomic instability. Aging Cell. 2002; 1:40–46. [PubMed: 12882352]

Liu M, Bandaru V, Bond JP, Jaruga P, Zhao X, Christov PP, Burrows CJ, Rizzo CJ, Dizdaroglu M, Wallace SS. The mouse ortholog of NEIL3 is a functional DNA glycosylase in vitro and in vivo. Proc Natl Acad Sci U S A. 2010; 107:4925–4930. [PubMed: 20185759]

Liu M, Bandaru V, Holmes A, Averill AM, Cannan W, Wallace SS. Expression and purification of active mouse and human NEIL3 proteins. Protein Expr Purif. 2012; 84:130–139. [PubMed: 22569481]

Liu M, Imamura K, Averill AM, Wallace SS, Doublie S. Structural characterization of a mouse ortholog of human NEIL3 with a marked preference for single-stranded DNA. Structure. 2013; 21:247–256. [PubMed: 23313161]

Madlener S, Strobel T, Vose S, Saydam O, Price BD, Demple B, Saydam N. Essential role for mammalian apurinic/apyrimidinic (AP) endonuclease Ape1/Ref-1 in telomere maintenance. Proc Natl Acad Sci U S A. 2013; 110:17844–17849. [PubMed: 24127576]

Massaad MJ, Zhou J, Tsuchimoto D, Chou J, Jabara H, Janssen E, Glauzy S, Olson BG, Morbach H, Ohsumi TK, et al. Deficiency of base excision repair enzyme NEIL3 drives increased predisposition to autoimmunity. J Clin Invest. 2016; 126:4219–4236. [PubMed: 27760045]

Meeker AK, Hicks JL, Platz EA, March GE, Bennett CJ, Delannoy MJ, De Marzo AM. Telomere shortening is an early somatic DNA alteration in human prostate tumorigenesis. Cancer Res. 2002; 62:6405–6409. [PubMed: 12438224]

Miller AS, Balakrishnan L, Buncher NA, Opresko PL, Bambara RA. Telomere proteins POT1, TRF1 and TRF2 augment long-patch base excision repair in vitro. Cell Cycle. 2012; 11:998–1007. [PubMed: 22336916]

Mjelle R, Hegre SA, Aas PA, Slupphaug G, Drablos F, Saetrom P, Krokan HE. Cell cycle regulation of human DNA repair and chromatin remodeling genes. DNA Repair (Amst). 2015; 30:53–67. [PubMed: 25881042]

Morland I, Rolseth V, Luna L, Rognes T, Bjoras M, Seeberg E. Human DNA glycosylases of the bacterial Fpg/MutM superfamily: an alternative pathway for the repair of 8-oxoguanine and other oxidation products in DNA. Nucleic Acids Res. 2002; 30:4926–4936. [PubMed: 12433996]

Muftuoglu M, Wong HK, Imam SZ, Wilson DM 3rd, Bohr VA, Opresko PL. Telomere repeat binding factor 2 interacts with base excision repair proteins and stimulates DNA synthesis by DNA polymerase beta. Cancer Res. 2006; 66:113–124. [PubMed: 16397223]

Neurauter CG, Luna L, Bjoras M. Release from quiescence stimulates the expression of human NEIL3 under the control of the Ras dependent ERK-MAP kinase pathway. DNA Repair (Amst). 2012; 11:401–409. [PubMed: 22365498]

Oikawa S, Kawanishi S. Site-specific DNA damage at GGG sequence by oxidative stress may accelerate telomere shortening. FEBS Lett. 1999; 453:365–368. [PubMed: 10405177]

Opresko PL, Fan J, Danzy S, Wilson DM 3rd, Bohr VA. Oxidative damage in telomeric DNA disrupts recognition by TRF1 and TRF2. Nucleic Acids Res. 2005; 33:1230–1239. [PubMed: 15731343]

Opresko PL, von Kobbe C, Laine JP, Harrigan J, Hickson ID, Bohr VA. Telomere-binding protein TRF2 binds to and stimulates the Werner and Bloom syndrome helicases. J Biol Chem. 2002; 277:41110–41119. [PubMed: 12181313]

Palm W, de Lange T. How shelterin protects mammalian telomeres. Annu Rev Genet. 2008; 42:301–334. [PubMed: 18680434]

Regnell CE, Hildrestrand GA, Sejersted Y, Medin T, Moldestad O, Rolseth V, Krokeide SZ, Suganthan R, Luna L, Bjoras M, et al. Hippocampal adult neurogenesis is maintained by Neil3-dependent repair of oxidative DNA lesions in neural progenitor cells. Cell Rep. 2012; 2:503–510. [PubMed: 22959434]

Reis A, Hermanson O. The DNA glycosylases OGG1 and NEIL3 influence differentiation potential, proliferation, and senescence-associated signs in neural stem cells. Biochem Biophys Res Commun. 2012; 423:621–626. [PubMed: 22564741]

Rolseth V, Krokeide SZ, Kunke D, Neurauter CG, Suganthan R, Sejersted Y, Hildrestrand GA, Bjoras M, Luna L. Loss of Neil3, the major DNA glycosylase activity for removal of hydantoins in single stranded DNA, reduces cellular proliferation and sensitizes cells to genotoxic stress. Biochim Biophys Acta. 2013; 1833:1157–1164. [PubMed: 23305905]

Rudolph P, Alm P, Olsson H, Heidebrecht HJ, Ferno M, Baldetorp B, Parwaresch R. Concurrent overexpression of p53 and c-erbB-2 correlates with accelerated cycling and concomitant poor prognosis in node-negative breast cancer. Hum Pathol. 2001; 32:311–319. [PubMed: 11274641]

Sejersted Y, Hildrestrand GA, Kunke D, Rolseth V, Krokeide SZ, Neurauter CG, Suganthan R, Atneosen-Asegg M, Fleming AM, Saugstad OD, et al. Endonuclease VIII-like 3 (Neil3) DNA glycosylase promotes neurogenesis induced by hypoxia-ischemia. Proc Natl Acad Sci U S A. 2011; 108:18802–18807. [PubMed: 22065741]

Semlow DR, Zhang J, Budzowska M, Drohat AC, Walter JC. Replication-Dependent Unhooking of DNA Interstrand Cross-Links by the NEIL3 Glycosylase. Cell. 2016; 167:498–511. e414. [PubMed: 27693351]

Torisu K, Tsuchimoto D, Ohnishi Y, Nakabeppu Y. Hematopoietic tissue-specific expression of mouse Neil3 for endonuclease VIII-like protein. J Biochem. 2005; 138:763–772. [PubMed: 16428305]

Vallabhaneni H, O'Callaghan N, Sidorova J, Liu Y. Defective repair of oxidative base lesions by the DNA glycosylase Nth1 associates with multiple telomere defects. PLoS Genet. 2013; 9:e1003639. [PubMed: 23874233]

van Steensel B, Smogorzewska A, de Lange T. TRF2 protects human telomeres from end-to-end fusions. Cell. 1998; 92:401–413. [PubMed: 9476899]

Verdun RE, Karlseder J. The DNA damage machinery and homologous recombination pathway act consecutively to protect human telomeres. Cell. 2006; 127:709–720. [PubMed: 17110331]

Wallace SS. Base excision repair: a critical player in many games. DNA Repair (Amst). 2014; 19:14–26. [PubMed: 24780558]

Wang Z, Rhee DB, Lu J, Bohr CT, Zhou F, Vallabhaneni H, de Souza-Pinto NC, Liu Y. Characterization of oxidative guanine damage and repair in mammalian telomeres. PLoS Genet. 2010; 6:e1000951. [PubMed: 20485567]

Wiederhold L, Leppard JB, Kedar P, Karimi-Busheri F, Rasouli-Nia A, Weinfeld M, Tomkinson AE, Izumi T, Prasad R, Wilson SH, et al. AP endonuclease-independent DNA base excision repair in human cells. Mol Cell. 2004; 15:209–220. [PubMed: 15260972]

Yang N, Galick H, Wallace SS. Attempted base excision repair of ionizing radiation damage in human lymphoblastoid cells produces lethal and mutagenic double strand breaks. DNA Repair (Amst). 2004; 3:1323–1334. [PubMed: 15336627]

Zhao Y, Sfeir AJ, Zou Y, Buseman CM, Chow TT, Shay JW, Wright WE. Telomere extension occurs at most chromosome ends and is uncoupled from fill-in in human cancer cells. Cell. 2009; 138:463–475. [PubMed: 19665970]

Zhou J, Fleming AM, Averill AM, Burrows CJ, Wallace SS. The NEIL glycosylases remove oxidized guanine lesions from telomeric and promoter quadruplex DNA structures. Nucleic Acids Res. 2015; 43:4039–4054. [PubMed: 25813041]

Zhou J, Liu M, Fleming AM, Burrows CJ, Wallace SS. Neil3 and NEIL1 DNA glycosylases remove oxidative damages from quadruplex DNA and exhibit preferences for lesions in the telomeric sequence context. J Biol Chem. 2013; 288:27263–27272. [PubMed: 23926102]

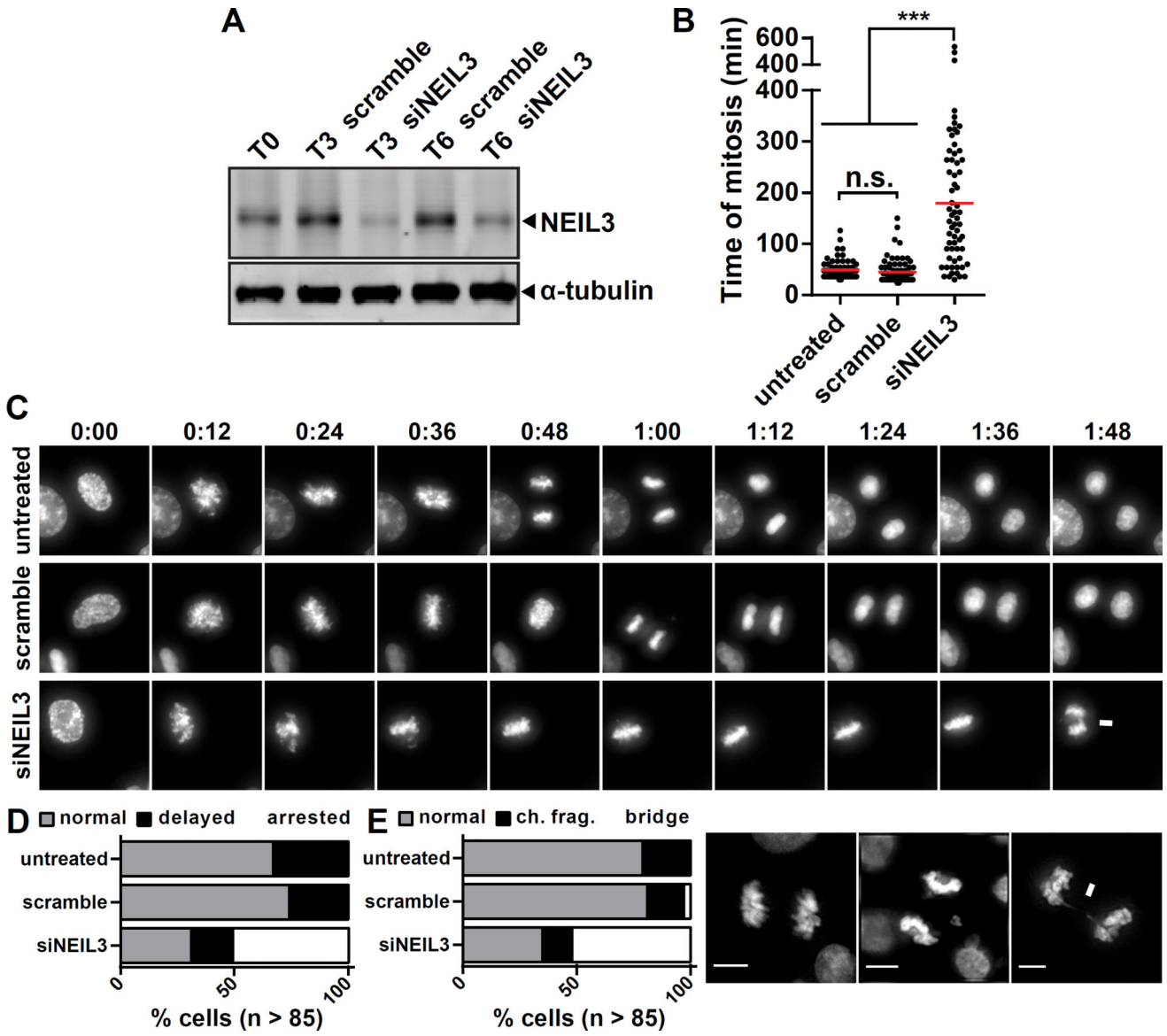

Figure 1. Knockdown of NEIL3 results in extended metaphase arrest and increases DNA bridging

(A) Western blot of NEIL3 immunoprecipitated from synchronized HCT116 cells treated with siRNAs. Lysates were harvested at indicated time points (hours) after release from the thymidine block. (B–C) Automated time-lapse microscopy of untreated, scramble-, or siNEIL3-treated HCT116 GFP-H2B cells after release from the thymidine block. (B) Dot plot of the total time from DNA condensation until chromatid separation from 3 pooled experiments (n > 60 cells; red line, average time of mitosis). (C) Representative projections of mitotic cells from Z-stacks imaged every 6 min over 16 h. Numbers represent time in minutes. (D–E) Histograms of normal versus aberrant mitotic timings (D) or DNA separation (E). (E) Representative micrographs of DNA separation are shown on the right (arrow head, chromosomal fragmentation; arrow, DNA bridge). Scale bar = 10 μm.

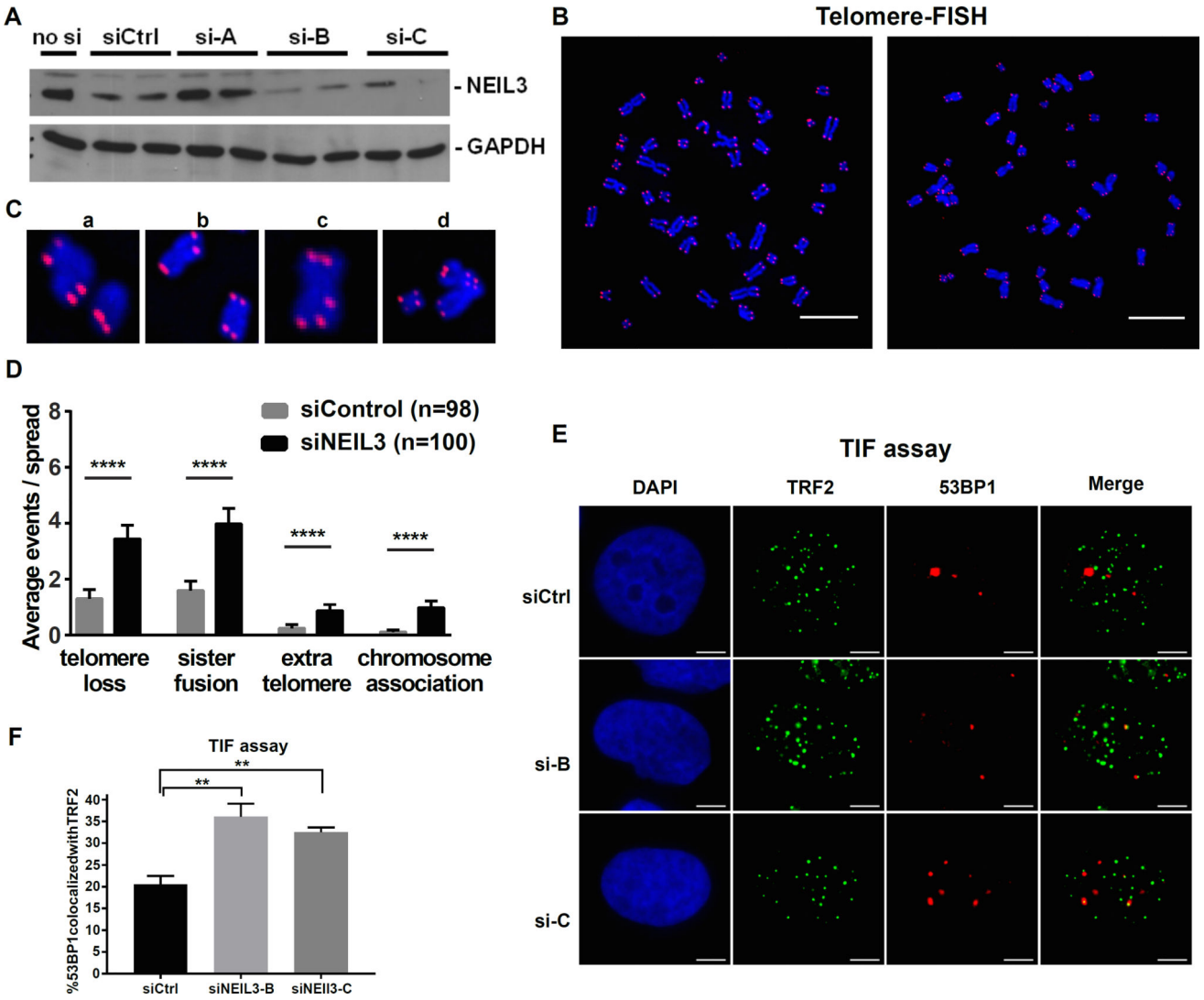

Figure 2. NEIL3 knockdown increases the occurrence of telomere dysfunction

(A) Western Blot shows successful knockdown of NEIL3 by si-B and si-C. Two independent knockdown experiments were shown. (B) Metaphase spreads of siControl- and siNEIL3-treated HCT116 cells. DNA was stained with DAPI (blue) and telomeres were labeled with Cy3-telomere PNA (red). White arrows indicate abnormal telomeres. Scale bars = 10 μm. (C) Representative micrographs of telomere defects: a) telomere loss, b) sister chromatid fusion, c) extra telomere signal, and d) chromosomal fusion. (D) Quantification of telomere defects. Mean and 95% confidence intervals are shown. (E) 53BP1 and TRF2 foci were visualized by immunofluorescence in siNEIL3-B, siNEIL3-C or control siRNA-treated U2OS cells. Scale bar = 5 μm. (F) Quantification of the images shows that siNEIL3-B and siNEIL3-C cells have increased TIFs. Three experiments were performed, imaged and quantified; and at least 50 cells with 53BP1 foci were counted in each experiment. **, $p < 0.005$, ****, $p < 0.0001$.

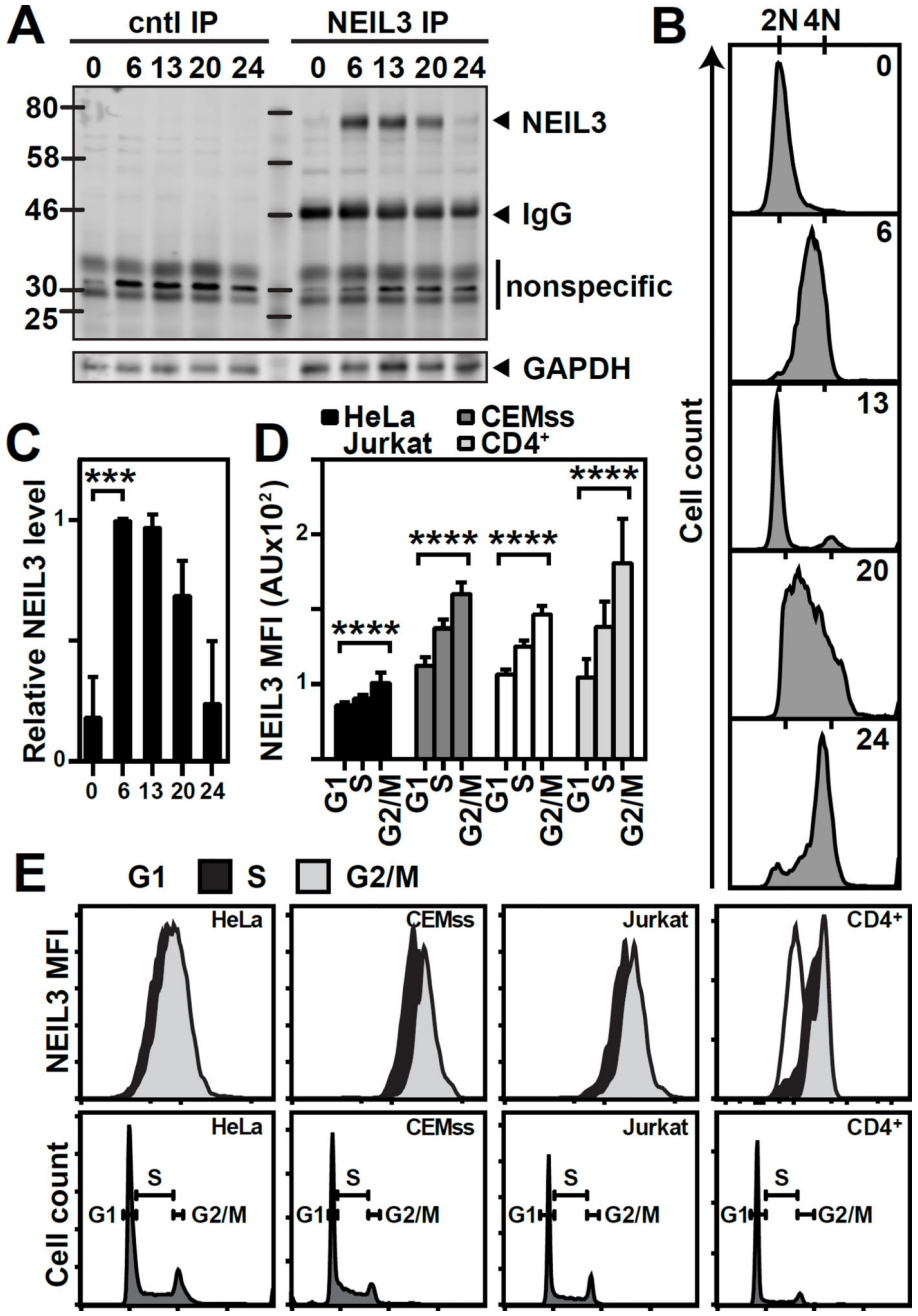

Figure 3. NEIL3 expression increases during S phase and reaches maximal levels in G2/M

(A–C) Analysis of NEIL3 levels in synchronized HeLa cells. (A) Western blot of NEIL3 immunoprecipitated from HeLa cells harvested over a 24 h time course. (B) Flow cytometry analyses of the relative DNA content were performed in parallel to determine cell cycle phase. (C) Quantification of immunoprecipitated NEIL3 levels normalized to cellular GAPDH (mean ± SD; n = 3; ***, $p \leq 0.001$). (D) Quantification of NEIL3 protein levels in asynchronous cell cultures (mean ± SD; n = 7; ****, $p \leq 0.0001$). (E) Representative flow cytometry profiles of NEIL3 protein levels (top row) relative to cell cycle phase as determined by relative DNA content (bottom row) in asynchronous cell cultures.

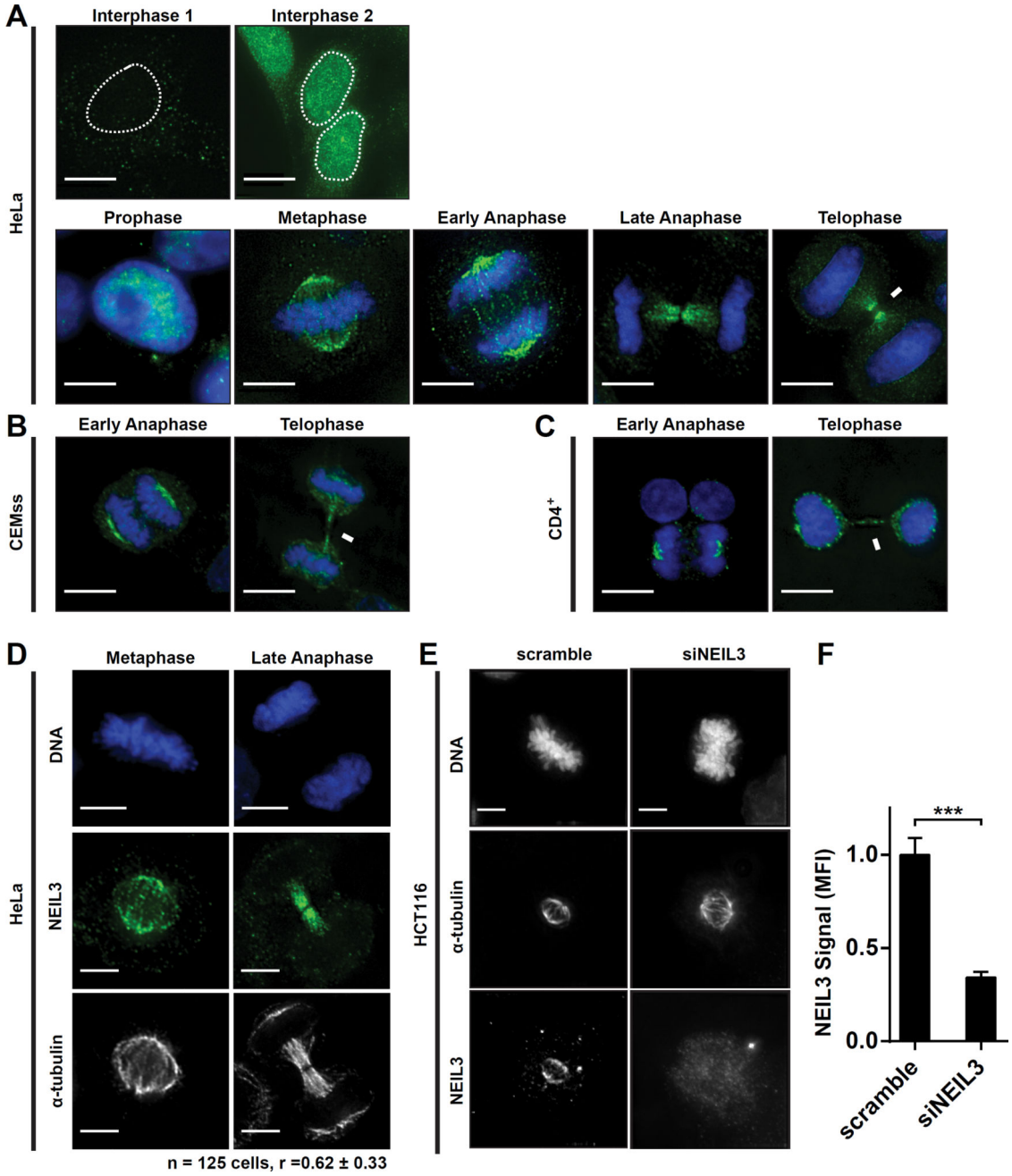

Figure 4. NEIL3 re-localizes from condensing DNA to spindle microtubules during mitosis

(A–C) Projections of deconvolved, whole cell Z-stacks of NEIL3 (green) in asynchronously dividing (A) HeLa cells, (B) CEMss cells, and (C) activated primary CD4+ T lymphocytes (n > 200 cells, pooled from 3 different passages). DNA (blue) was stained with DAPI. Dotted lines denote the nuclear boundary; arrows indicate the abscission zone. (D) Deconvolution micrographs of a single focal plain containing the poles of the mitotic spindle or the intercellular bridge were used for Pearson's co-localization analysis (r) of NEIL3 (green) and α-tubulin (white) in asynchronous HeLa cells (mean ± SD; n = total cells pooled from 3 independent experiments). (E) Projections from deconvolution Z-stacks of metaphase

HCT116 GFP-H2B cells. Scramble- (left) and siNEIL3- (right) treated cells were stained for NEIL3 (SC-50749) and α-tubulin. Scale bar = 5 μm. (F) Quantification of NEIL3 knockdown was calculated using the MFI of NEIL3 normalized to α-tubulin (mean ± SD; n = 3 independent replicates; ***, $p < 0.001$).

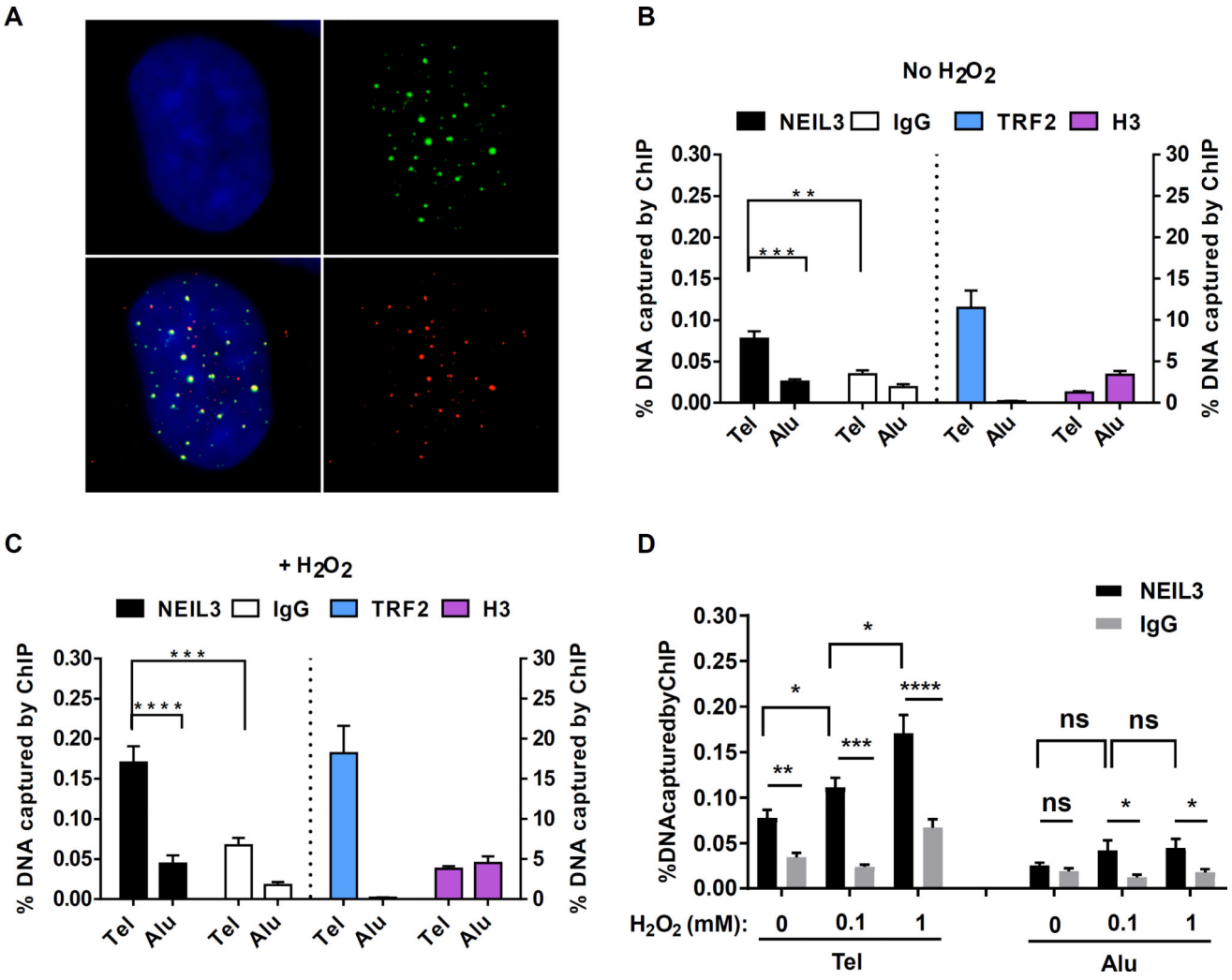

Figure 5. NEIL3 localizes to telomeres and the localization increases following H^2O^2 treatment during S phase

(A) A representative image of immunofluorescence showing that NEIL3 (green) co-localizes to TRF2 (red) in U2OS cells. Scale bar = 5 μm. More images can be found in Figure S2 and Figure S3. (B) Telomere DNA captured by ChIP and quantified by qPCR without H_2O_2 treatment. HeLa cells were synchronized by thymidine block and cells were cross-linked 6 hours after release to use for ChIP. The percentage of DNA captured was calculated by normalizing to a 2% input using Ct values. (C) Telomere DNA captured by ChIP and quantified by qPCR following H_2O_2 treatment. The same protocol was used as in (B), except that HeLa cells were treated with 1 mM H_2O_2 in PBS at 37°C for 15 min and recovered in fresh medium for 2.75 hours before cross-linking. (D) Dose dependency of NEIL3 recruitment to telomeres. The same protocol was used as in (C), with the difference being the H_2O_2 concentration used. Each bar represents a minimum of three individual ChIP experiments and two qPCR reactions for each ChIP sample. Mean and standard deviation are shown. (**, $p < 0.01$, ***, $p < 0.001$, ****, $p < 0.0001$).

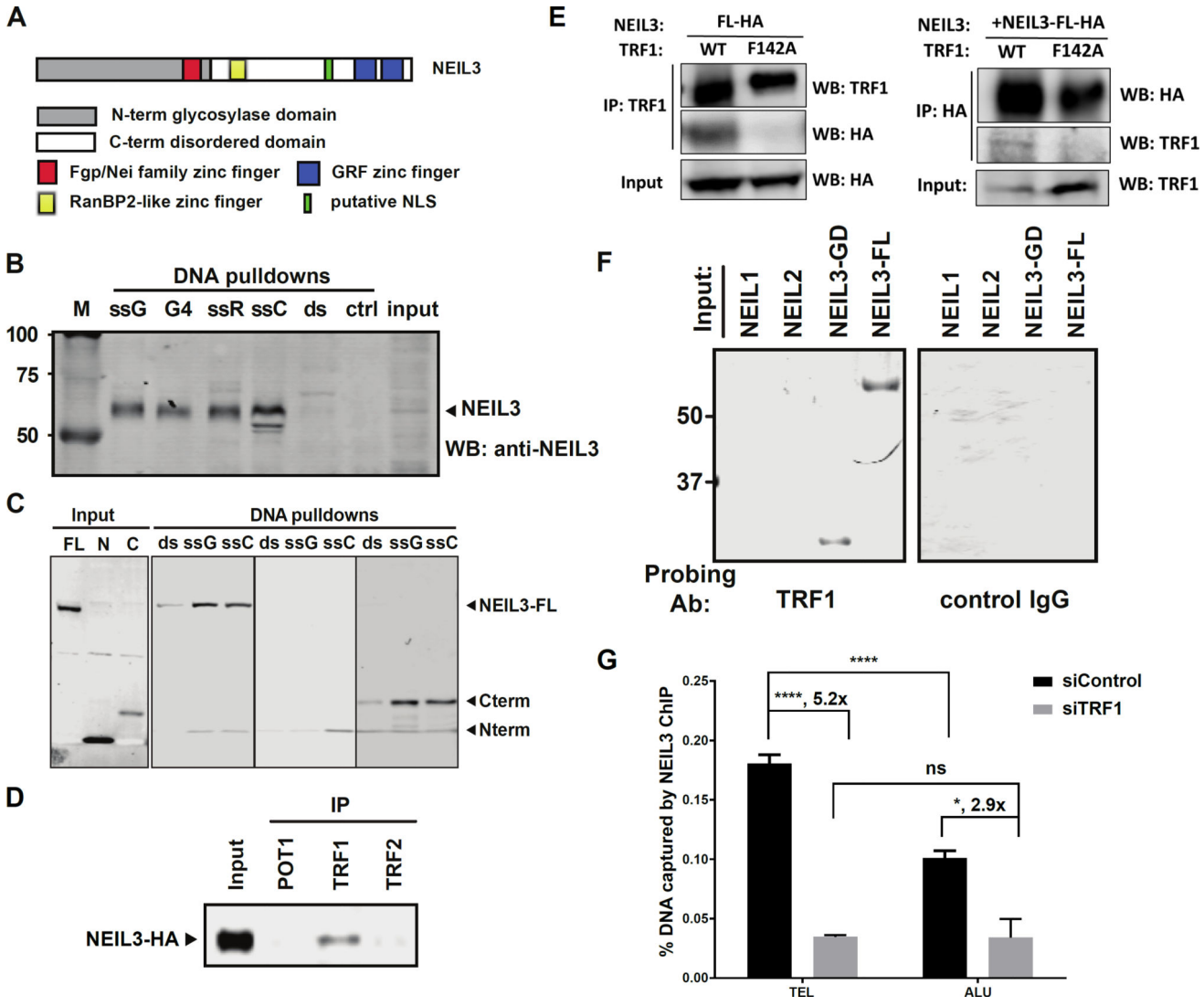

Figure 6. NEIL3 binds to single-stranded DNA in a sequence non-specific manner

(A) Domains and motifs of the NEIL3 protein. NEIL3 contains a conserved N-term glycosylase domain and a large intrinsically disordered domain with unknown function. (B) The endogenous NEIL3 protein binds to ssDNA and quadruplex DNA (but not dsDNA) in a sequence independent manner. To perform DNA pulldown assays, biotinylated telomeric double-stranded (ds), single-stranded (ssG or ssC), or quadruplex DNA (G4) were incubated with HeLa cell lysates. (C) The CTD of NEIL3 is responsible for ssDNA binding. Lysates from HEK293T cells transfected with HA-tagged NEIL3 constructs were incubated with biotinylated DNA oligos. A representative Western blot of three independent pulldowns is shown. (D) Co-immunoprecipitation experiment using TRF1, TRF2 and POT1 antibodies in a lysate of NEIL3-HA transfected HEK293T cells. NEIL3-HA was detected by blotting with an anti-HA antibody. (E) NEIL3 co-immunoprecipitated with WT TRF1 but not F142A mutation. Left, HEK293T cells were transfected with HA-tagged NEIL3 and TRF1 constructs. WT TRF1 and TRFH domain mutant F142A were immunoprecipitated and the immunoprecipitants were subjected to Western blot detection for HA-tagged NEIL3. Right,

the reverse co-immunoprecipitation. NEIL3-HA was immunoprecipitated and the immunoprecipitants were subjected to Western blot detection for TRF1. (F) Representative Far-Western blot revealing the interaction of NEIL3 with TRF1. (G) Binding of NEIL3 to telomeres was greatly reduced when TRF1 was knocked down. *, $p < 0.05$, ****, $p < 0.0001$, ns, not significantly different.

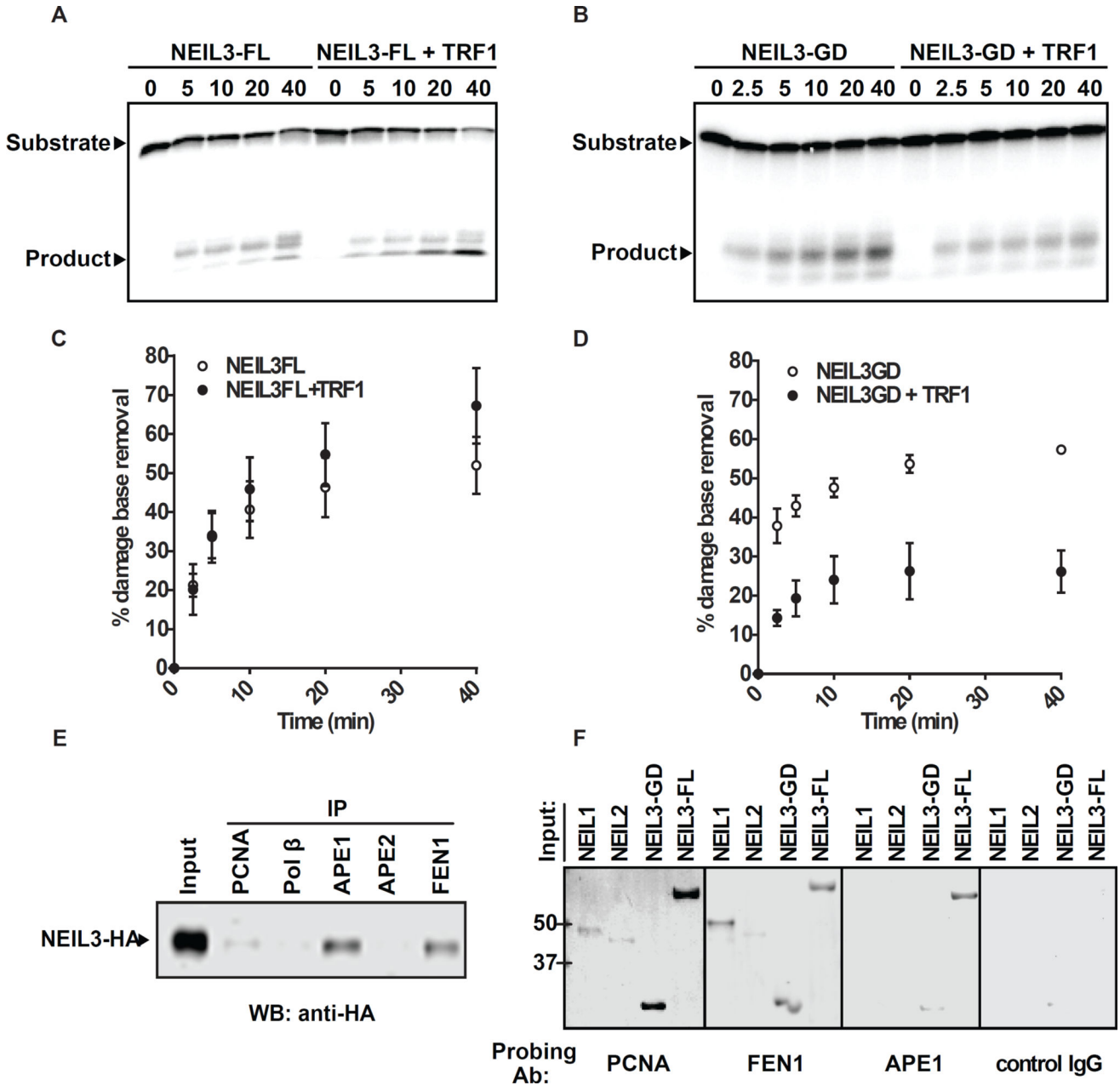

Figure 7. The CTD of NEIL3 interacts with TRF1 and LP-BER proteins PCNA, FEN1, and APE1 and is required for optimal NEIL3 activity

(A–B) Radiographs of glycosylase assays in the presence or absence of TRF1. Duplex telomere DNA containing an oxidative lesion (Gh) was incubated with purified (A) NEIL3-FL or (B) NEIL3-GD. Reactions were stopped at the indicated time in minutes. (C–D) Quantification of the effect of TRF1 on the enzymatic activity of (C) NEIL3-FL or (D) NEIL3-GD. (E) Co-immunoprecipitation reveals interactions between NEIL3 and components of LP-BER pathways. BER proteins were pulled down from HEK293T cell lysates expressing NEIL3-HA, and the presence of NEIL3 was detected via the HA epitope. (B) Far-Western blots analyzing the interaction between the purified NEIL proteins and LP-BER proteins. The NEIL proteins were loaded on to PAGE and transferred to a PVDF

membrane. The proteins were refolded on the membrane and incubated with a HeLa whole cell extract. Antibodies against the indicated proteins were used to detect the interactions.